

Effects of initial stresses on guided waves in unidirectional plates

X. M. ZHANG, J. G. YU

*School of Mechanical and Power Engineering
Henan Polytechnic University
454003, Jiaozuo, P.R. China
e-mails: zxmworld11@hpu.edu.cn,
yu@emails.bjut.edu.cn*

THE GUIDED WAVE PROPAGATION IN UNIDIRECTIONAL PLATES under gravity, homogeneous initial stress in the thickness direction and inhomogeneous initial stress in the wave propagating direction is investigated in this paper based on the theory of mechanics of incremental deformations. The Legendre orthogonal polynomial series expansion method is used to solve the coupled wave equation. Two different wave propagating directions, the fiber orientation and the vertical fiber orientation, are discussed respectively. The effects of the initial stresses on the Lamb-like wave and shear-horizontal (SH) wave are respectively investigated. The effects of the initial stresses on the dispersion curves and on the displacement and stress distributions are discussed.

Key words: initial stress, unidirectional plates, guided wave, dispersion curves, displacement and stress distributions.

Copyright © 2013 by IPPT PAN

1. Introduction

IN MANY PRACTICAL APPLICATIONS, initial stresses are present due to mechanical loads or thermal fields or could arise as residual stresses in casting, forging or other manufacturing processes. It is well known that an initial stress state in a body can significantly affect its mechanical behavior. The propagation of elastic waves in a composite structure with initial stresses has long been of interest, and some achievements have been reported. Taking into account the effect of initial stresses and using Biot's theory of incremental deformations [1], DEY [2] modified the work of JONES [3]. ROY [4] studied the wave propagation in a thin two-layered laminated medium with stress couples under initial stresses. ABD-ALLA and AHMED [5] investigated the Love wave propagation in a non-homogeneous orthotropic elastic layer under the initial stress overlying semi-infinite medium. GARG [6] considered the effect of initial stress on harmonic plane homogeneous waves in viscoelastic anisotropic media. MONTANARO [7] studied the wave prop-

agation along symmetry axes in linearly elastic media with an initial stress. GUZ [8] developed a method to measure the biaxial homogeneous initial stress field in the elastic body using elastic waves. AKBAROV and OZISIK [9] investigated the influence of the third order elastic constants to the generalized Rayleigh wave dispersion in a pre-stressed stratified half-plane. GUPTA *et al.* [10] investigated the torsional surface waves in a homogeneous layer of finite thickness over an initially stressed heterogeneous half-space. SINGH [11] studied the wave propagation in a pre-stressed piezoelectric half-space. AKBAROV and GULIEV [12] studied axisymmetric longitudinal wave in a pre-strained compound circular cylinder made from compressible materials. AKBAROV *et al.* [13] studied the torsional wave in a finitely pre-strained hollow sandwich circular cylinder. AKBAROV and GULIEV [14] also investigated the influence of the finite initial strains on the axisymmetric wave dispersion in a circular cylinder embedded in a compressible elastic medium.

As common structures, initial stressed plates are also given attention in the wave propagation studies. KAYESTHA and WIJEYEWICKREMA [15] studied time-harmonic wave propagation in a pre-stressed compressible elastic bi-material laminate and obtained dispersion curves. AKBAROV *et al.* [16] and ZAMANOV and AGASIYEV [17] studied the influence of the initial strains in the wave propagation direction on the Lamb wave dispersion curves. AKBAROV *et al.* [18] also studied the influence of the initial strains in the thickness direction on the Lamb wave dispersion curves. In this paper, the guided wave propagation in unidirectional plates under gravity, initial stresses in the thickness and the wave propagating directions are studied based on the mechanics of incremental deformations [1]. The coupled wave equation is solved by the Legendre orthogonal polynomial series expansion method. The effects on the Lamb-like wave and SH wave are investigated respectively. Two different wave propagating directions, in fiber orientation and the vertical fiber orientation are discussed respectively. The numerical results are presented and discussed to illustrate the effects of the initial stresses on the dispersion curves, displacement and stress distributions.

2. Theoretical formulation

Consider a unidirectional plate with initial stresses in two directions,

$$S_{xx} = -P(z) \quad \text{and} \quad S_{zz} = -Q,$$

as shown in Fig. 1. The plate is infinite horizontally with a thickness h . We place the horizontal (x,y) -plane of a Cartesian coordinate system on the bottom surface and let the plate be in the positive z -region.

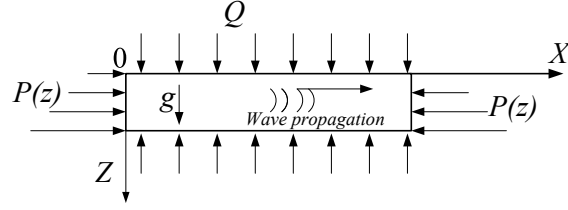


FIG. 1. Schematic diagram of wave propagation in a plate under initial stresses and gravity.

According to “Mechanics of Incremental Deformations” [1, 19], the dynamic equation for the unidirectional plate under gravity and initial stresses is governed by

$$\begin{aligned}
 (2.1) \quad & \frac{\partial T_{xx}}{\partial x} + \frac{\partial T_{xy}}{\partial y} + \frac{\partial T_{xz}}{\partial z} - \frac{1}{2} \left(\frac{\partial u_x}{\partial z} + \frac{\partial u_z}{\partial x} \right) \frac{\partial S_{xx}}{\partial z} \\
 & \quad + S_{xx} \frac{\partial \omega_z}{\partial y} + (S_{zz} - S_{xx}) \frac{\partial \omega_y}{\partial z} + \rho g \frac{\partial u_z}{\partial x} = \rho \frac{\partial^2 u_x}{\partial t^2}, \\
 & \frac{\partial T_{xy}}{\partial x} + \frac{\partial T_{yy}}{\partial y} + \frac{\partial T_{yz}}{\partial z} - S_{zz} \frac{\partial \omega_x}{\partial z} + S_{xx} \frac{\partial \omega_z}{\partial x} = \rho \frac{\partial^2 u_y}{\partial t^2}, \\
 & \frac{\partial T_{xz}}{\partial x} + \frac{\partial T_{yz}}{\partial y} + \frac{\partial T_{zz}}{\partial z} + (S_{zz} - S_{xx}) \frac{\partial \omega_y}{\partial x} - S_{zz} \frac{\partial \omega_x}{\partial y} - \rho g \frac{\partial u_x}{\partial x} = \rho \frac{\partial^2 u_z}{\partial t^2},
 \end{aligned}$$

where

$$\begin{aligned}
 \omega_x &= \frac{1}{2} \left(\frac{\partial u_z}{\partial y} - \frac{\partial u_y}{\partial z} \right), \\
 \omega_y &= \frac{1}{2} \left(\frac{\partial u_x}{\partial z} - \frac{\partial u_z}{\partial x} \right), \\
 \omega_z &= \frac{1}{2} \left(\frac{\partial u_y}{\partial x} - \frac{\partial u_x}{\partial y} \right).
 \end{aligned}$$

The constitutive equation for the unidirectional plate can be written in the following form:

$$(2.2) \quad \begin{Bmatrix} T_{xx} \\ T_{yy} \\ T_{zz} \\ T_{yz} \\ T_{xz} \\ T_{xy} \end{Bmatrix} = \begin{bmatrix} C_{11} - S_{xx} & C_{12} - S_{xx} & C_{13} - S_{xx} & 0 & 0 & 0 \\ C_{12} & C_{22} & C_{23} & 0 & 0 & 0 \\ C_{13} - S_{zz} & C_{23} - S_{zz} & C_{33} - S_{zz} & 0 & 0 & 0 \\ 0 & 0 & 0 & C_{44} & 0 & 0 \\ 0 & 0 & 0 & 0 & C_{55} & 0 \\ 0 & 0 & 0 & 0 & 0 & C_{66} \end{bmatrix} \begin{Bmatrix} \varepsilon_{xx} \\ \varepsilon_{yy} \\ \varepsilon_{zz} \\ 2\varepsilon_{yz} \\ 2\varepsilon_{xz} \\ 2\varepsilon_{xy} \end{Bmatrix} \pi(z),$$

where $\pi(z)$ is the rectangular window function defined by

$$\pi(z) = \begin{cases} 1, & 0 \leq z \leq h, \\ 0, & \text{elsewhere,} \end{cases}$$

whose derivative is $\delta(z-0) - \delta(z-h)$, which is introduced so as to meet the stress-free boundary conditions ($T_{xz} = T_{yz} = T_{zz} = 0$ at $z = 0, z = h$).

The relationship between the strain and displacement can be expressed as

$$(2.3) \quad \begin{aligned} \varepsilon_{xx} &= \frac{\partial u_x}{\partial x}, & \varepsilon_{yy} &= \frac{\partial u_y}{\partial y}, & \varepsilon_{zz} &= \frac{\partial u_z}{\partial z}, \\ \varepsilon_{yz} &= \frac{1}{2} \left(\frac{\partial u_y}{\partial z} + \frac{\partial u_z}{\partial y} \right), \\ \varepsilon_{xz} &= \frac{1}{2} \left(\frac{\partial u_x}{\partial z} + \frac{\partial u_z}{\partial x} \right), \\ \varepsilon_{xy} &= \frac{1}{2} \left(\frac{\partial u_x}{\partial y} + \frac{\partial u_y}{\partial x} \right). \end{aligned}$$

Here $u_i, T_{ij}, \varepsilon_{ij}$ are the elastic displacements, stresses and strains; C_{ij} are the elastic coefficients; ρ is the density of the plate.

For a free harmonic wave being propagated in the x direction, we assume displacement components to be of the form:

$$(2.4) \quad u_x(x, y, z, t) = \exp(ikx - i\omega t)U(z),$$

$$(2.5) \quad u_y(x, y, z, t) = \exp(ikx - i\omega t)V(z),$$

$$(2.6) \quad u_z(x, y, z, t) = \exp(ikx - i\omega t)W(z).$$

$U(z), V(z), W(z)$ represent the amplitudes of vibration in the x, y, z directions; k is the magnitude of the wave vector in the propagation direction, and ω is the angular frequency.

Substituting Eqs. (2.2)–(2.6) into Eq. (2.1), governing differential equations in terms of displacement components can be obtained:

$$(2.7) \quad \begin{aligned} & [C_{55}U'' + ik(C_{13} + C_{55} + 0.5P + 0.5Q)W' + 0.5(P - Q)U'' \\ & + 0.5P'U' + 0.5ikP'W - k^2(C_{11} + P)U + ik\rho gW]\pi(z) \\ & + (\delta(z-0) - \delta(z-h))(C_{55}U' + ikC_{55}W) \\ & = -\rho\omega^2U\pi(z), \end{aligned}$$

$$(2.8) \quad \begin{aligned} & [C_{44}V'' - 0.5QV'' - k^2(C_{66} - 0.5P)V]\pi(z) \\ & + (\delta(z-0) - \delta(z-h))C_{44}V' \\ & = -\rho\omega^2V\pi(z), \end{aligned}$$

$$\begin{aligned}
(2.9) \quad & [(C_{33} + Q)W'' + ik(C_{13} + C_{55} + 0.5P + 0.5Q)U' \\
& - k^2(C_{55} - 0.5P + 0.5Q)W - ik\rho gU]\pi(z) \\
& + (\delta(z - 0) - \delta(z - h))[(C_{33} + Q)W' + ik(C_{13} + Q)U] \\
& = -\rho\omega^2 W\pi(z).
\end{aligned}$$

Here, Eq. (2.8) is independent of other two equations and represents the propagating SH waves. Equations (2.7) and (2.9) control the propagating Lamb-like waves; they can be solved respectively. Next, the Lamb-like wave equations are solved firstly.

To obtain the solutions of the Lamb-like waves controlled by the coupled Eqs. (2.7) and (2.9), we expand $U(z)$ and $W(z)$ to a Legendre orthogonal polynomial series as

$$\begin{aligned}
(2.10) \quad & U(z) = \sum_{m=0}^{\infty} p_m^1 Q_m(z), \\
& W(z) = \sum_{m=0}^{\infty} p_m^2 Q_m(z),
\end{aligned}$$

where p_m^i ($i = 1, 2$) is the expansion coefficients and

$$Q_m(z) = \sqrt{\frac{2m+1}{h}} P_m\left(\frac{2z-h}{h}\right),$$

with P_m being the m -th Legendre polynomial. Theoretically, m runs from 0 to ∞ . In practice, the summation over the polynomials in Eq. (2.10) can be halted at some finite value $m = M$, when higher order terms become essentially negligible.

Equations (2.7)–(2.9) are multiplied by $Q_j(z)$ with j running from 0 to M . Then integrating over z from 0 to h gives the following $2(M+1)$ equations:

$$(2.11) \quad \begin{bmatrix} A_{11}^{j,m} & A_{12}^{j,m} \\ A_{21}^{j,m} & A_{22}^{j,m} \end{bmatrix} \begin{Bmatrix} p_m^1 \\ p_m^2 \end{Bmatrix} = -\rho\omega^2 \begin{bmatrix} M_m^j & 0 \\ 0 & M_m^j \end{bmatrix} \begin{Bmatrix} p_m^1 \\ p_m^2 \end{Bmatrix},$$

where $A_{\alpha\beta}^{j,m}$ ($\alpha, \beta = 1, 2$) and M_m^j are the elements of a non-symmetric matrix. They can be obtained according to Eqs. (2.7)–(2.9) and are given in the Appendix.

Equation (2.11) can be rewritten compactly as

$$(2.12) \quad [M^{-1}A]_{j,m}^{\alpha,\beta} p_m^\beta = -\omega^2 p_j^\alpha,$$

where the eigenvalue ω^2 gives the angular frequency of the guided wave and eigenvectors p_j^α allow the components of the particle displacement to be calculated. Using equation $V_{ph} = \omega/k$, the phase velocity can be obtained. The complex matrix Eq. (2.12) can be solved numerically by making use of standard computer programs for the diagonalization of non-symmetric square matrices. $2(M + 1)$ eigenmodes are generated from the order M of the expansion. Acceptable solutions are those eigenmodes for which convergence is obtained as M is increased. It was determined that the obtained eigenvalues are converged solutions when a further increase in the matrix dimension does not result in a significant change in the eigenvalue. The computer program was written using Mathematica.

The procedure of solving the SH wave equation (2.8) is similar to that of solving Lamb-like waves, but it is simpler and it is not presented here.

3. Numerical results

Based on the foregoing formulation, a computer program has been written to calculate the dispersion curves, displacement and stress distributions for the unidirectional plate with initial stresses. In order to illustrate the effect of the initial stress, two different wave propagating directions in fiber orientation and the vertical fiber orientation are discussed respectively. The numerical examples are discussed under four conditions:

- (a) x -direction initial stress and wave propagating in fiber orientation;
- (b) x -direction initial stress and wave propagating in the vertical fiber orientation;
- (c) z -direction initial stress and wave propagating in fiber orientation;
- (d) z -direction initial stress and wave propagating in the vertical fiber orientation.

The material properties of the unidirectional plate are given directly according to the literature [20], as shown in Table 1.

Table 1. The material properties of the unidirectional plate.

Property	C_{11}	C_{13}	C_{33}	C_{44}	C_{55}	C_{66}	ρ
x -direction in fiber orientation	128.2	6.9	14.95	3.81	6.73	6.73	1.58
x -direction in the vertical fiber orientation	14.95	7.33	14.95	6.73	3.81	6.73	1.58

Units: C_{ij} (10^9 N/m²), ρ (10^3 kg/m³).

3.1. Convergence of the polynomial series method

In this section, we firstly make a comparison between the results of the SH wave obtained by employing the polynomial approach and the corresponding ones obtained by employing the exact solution to the governing field equation to illuminate the validity of the polynomial approach. Then, the Lamb-like wave dispersion curves for the unidirectional plate under homogeneous initial stress P are calculated for different “ M ” to verify the constringency of the polynomial approach.

Without considering the boundary conditions, Eq. (2.8) can be written as

$$(3.1) \quad C_{44}V'' - 0.5QV'' - k^2C_{66}V = -\rho\omega^2V\pi(z).$$

The general solution is

$$(3.2) \quad V(z) = A \sin \left[\frac{z\sqrt{\rho\omega^2 - k^2C_{66}}}{\sqrt{C_{44} - 0.5Q}} \right] + B \cos \left[\frac{z\sqrt{\rho\omega^2 - k^2C_{66}}}{\sqrt{C_{44} - 0.5Q}} \right],$$

where A and B are undetermined coefficients.

Substituting Eq. (2.14) into the stress-free boundary condition ($T_{yz} = 0$ at $z = 0, z = h$), the SH wave dispersion equation can be obtained:

$$(3.3) \quad \frac{\rho\omega^2 - k^2C_{66}}{C_{44} - 0.5Q} \sin \left[\frac{h\sqrt{\rho\omega^2 - k^2C_{66}}}{\sqrt{C_{44} - 0.5Q}} \right] = 0.$$

We use the polynomial method to calculate the SH wave dispersion equation for the unidirectional plate with the wave propagating in vertical fiber orientation under homogeneous initial stress $Q = -3$ GPa and make a comparison with the exact solutions to the governing field equation, as shown in Fig. 2. It can be seen that the first four modes are coinciding when $M = 7$; the first five modes are coinciding when $M = 8$ and the first seven modes are coinciding when $M = 9$. So, we can conclude that the polynomial method’s results and the exact results agree very well at at least the first $(M + 1)/2$ modes.

In order to verify the constringency of the polynomial series method, the Lamb-like wave dispersion curves for the unidirectional plate with the wave propagating in fiber orientation under homogeneous initial stress $P = -3$ GPa are calculated when $M = 7, 8, 9$ and 10 , respectively, as shown in Fig. 3. It can be noticed that the first four modes are convergent when $M = 7$; the first five modes are convergent when $M = 8$ and the first six modes are convergent when $M = 9$. So, we can think that at least the first $(M + 1)/2$ modes are convergent.

For all the undermentioned calculations, the series expansion is truncated at $M = 12$.

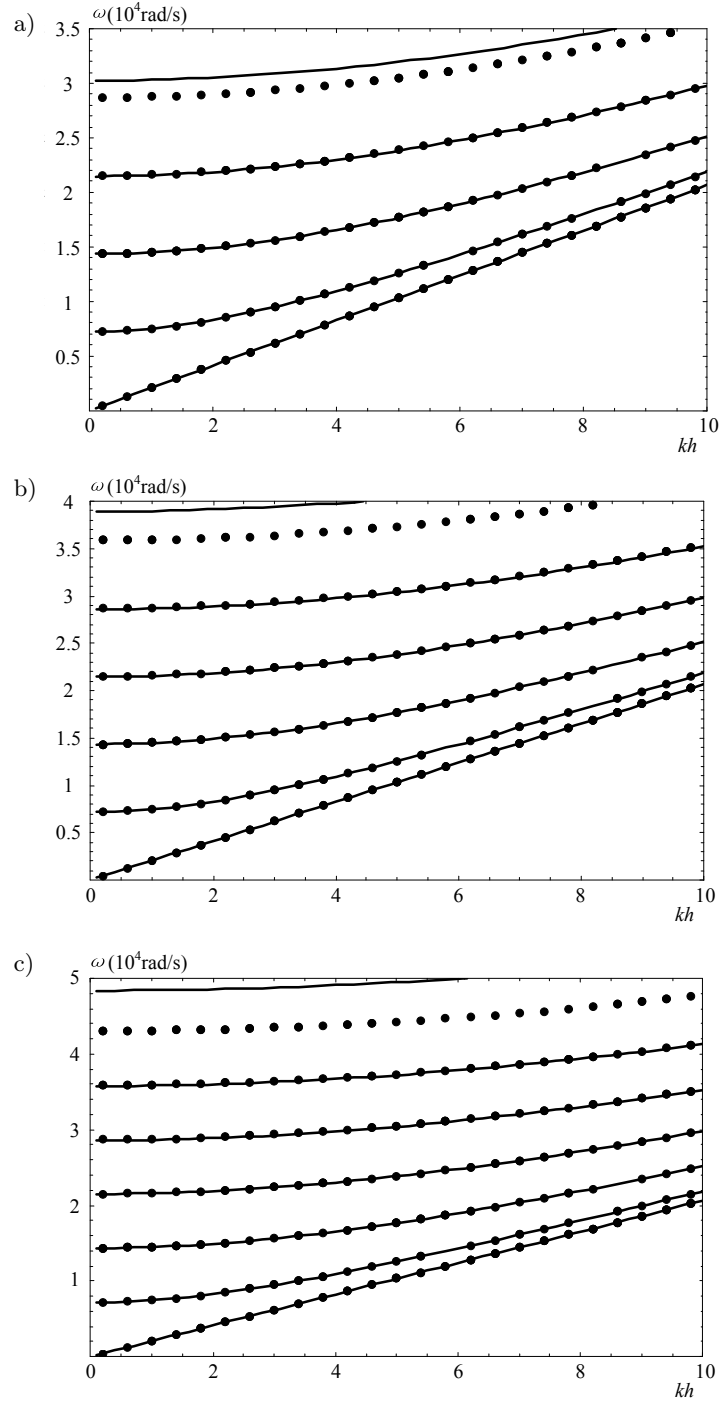


FIG. 2. Dispersion curves for SH wave under homogeneous initial stress $Q = -3$ GPa; dots: the exact results, lines: polynomial method's results; a) $M = 7$, b) $M = 8$, c) $M = 9$.

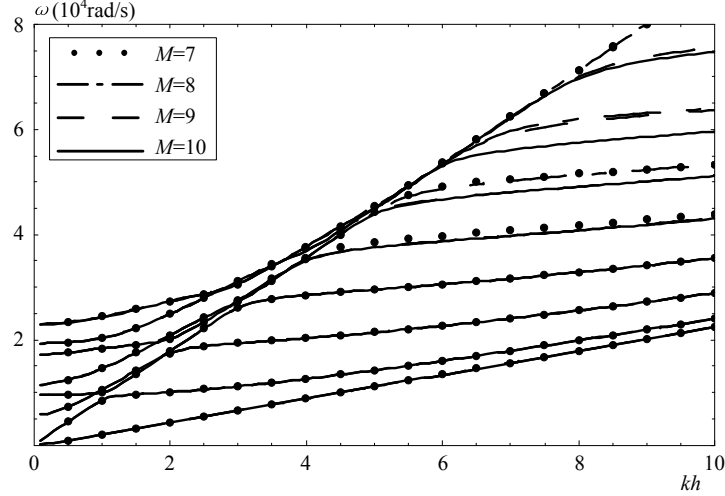


FIG. 3. Dispersion curves for Lamb-like wave under homogeneous initial stress $P = -3$ GPa for various “ M ”.

3.2. Effects of the gravity and initial stresses on the Lamb-like wave dispersion curves

Figure 4 shows the phase velocity dispersion curves of the unidirectional plate with the wave propagating in fiber orientation and the vertical fiber orientation under gravity and different homogeneous initial stresses P . It can be seen that the gravity has no influence on the Lamb-like wave dispersion curves. A stretch stress always makes the wave speed higher at low frequencies (except for the first mode). In most cases, the effect of the compressive stress is contrary to that of the stretch stress. Comparing Fig. 4a and Fig. 4b, we can see that when the wave propagates in fiber orientation, the effect of the initial stress P on the anti-symmetrical modes is more significant than that on the symmetrical modes at low frequencies which is more obvious at low order modes. But when the wave propagates in the vertical fiber orientation, the effects on the symmetrical modes and the anti-symmetrical modes have no significant differences.

Figure 5 shows the phase velocity dispersion curves of the unidirectional plate under different initial stresses Q . It can be seen that the effect of the initial stress Q is very different from that of the initial stress P . For the first three modes, the effect of the initial stress Q is almost entirely contrary to that of initial stress P . Moreover, the effect of the initial stress Q on the symmetrical modes is contrary to that on the anti-symmetrical modes at low frequencies when the wave propagates in fiber orientation. But the effect on the symmetrical modes

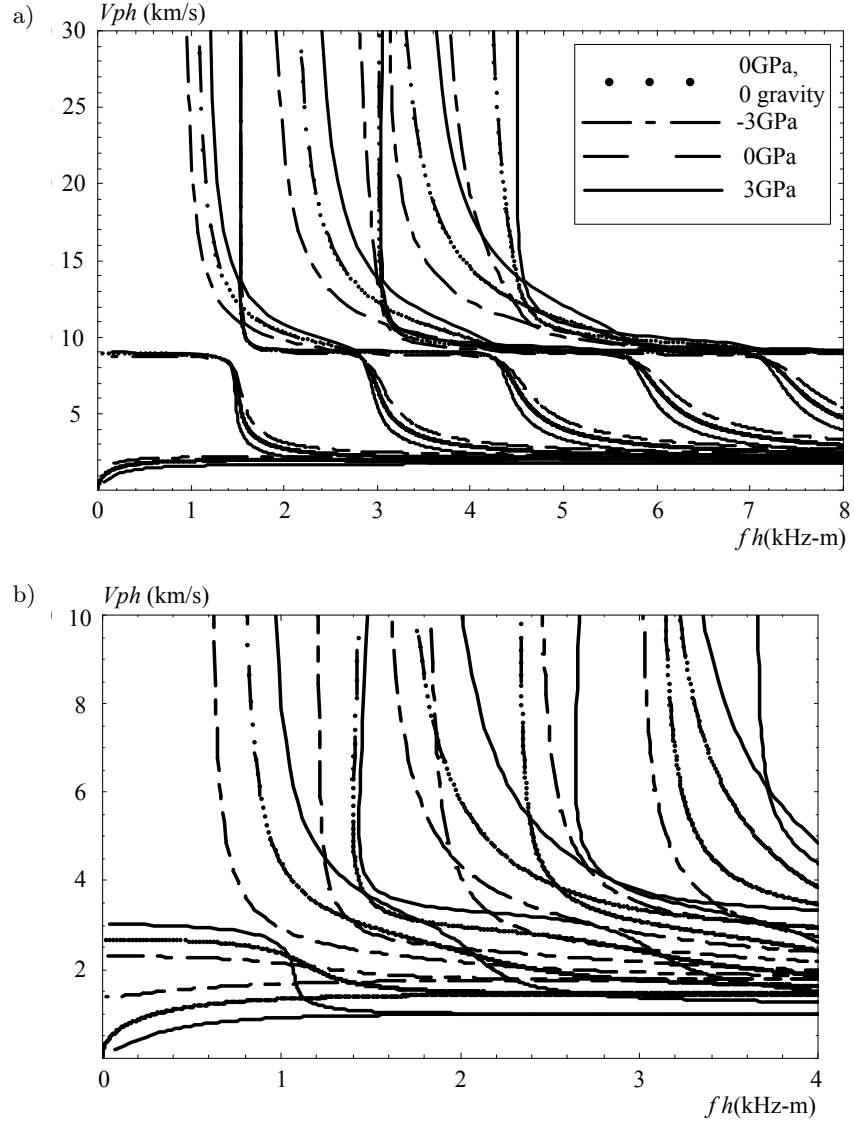


FIG. 4. Phase velocity spectra for the unidirectional plate under different homogeneous initial stresses P : a) wave propagating in fiber orientation, b) wave propagating in the vertical fiber orientation.

is similar to that on the anti-symmetrical modes when the wave propagates in the vertical fiber orientation.

Figure 6 shows the phase velocity dispersion curves of the unidirectional plate with the wave propagating in fiber orientation under two different initial stresses

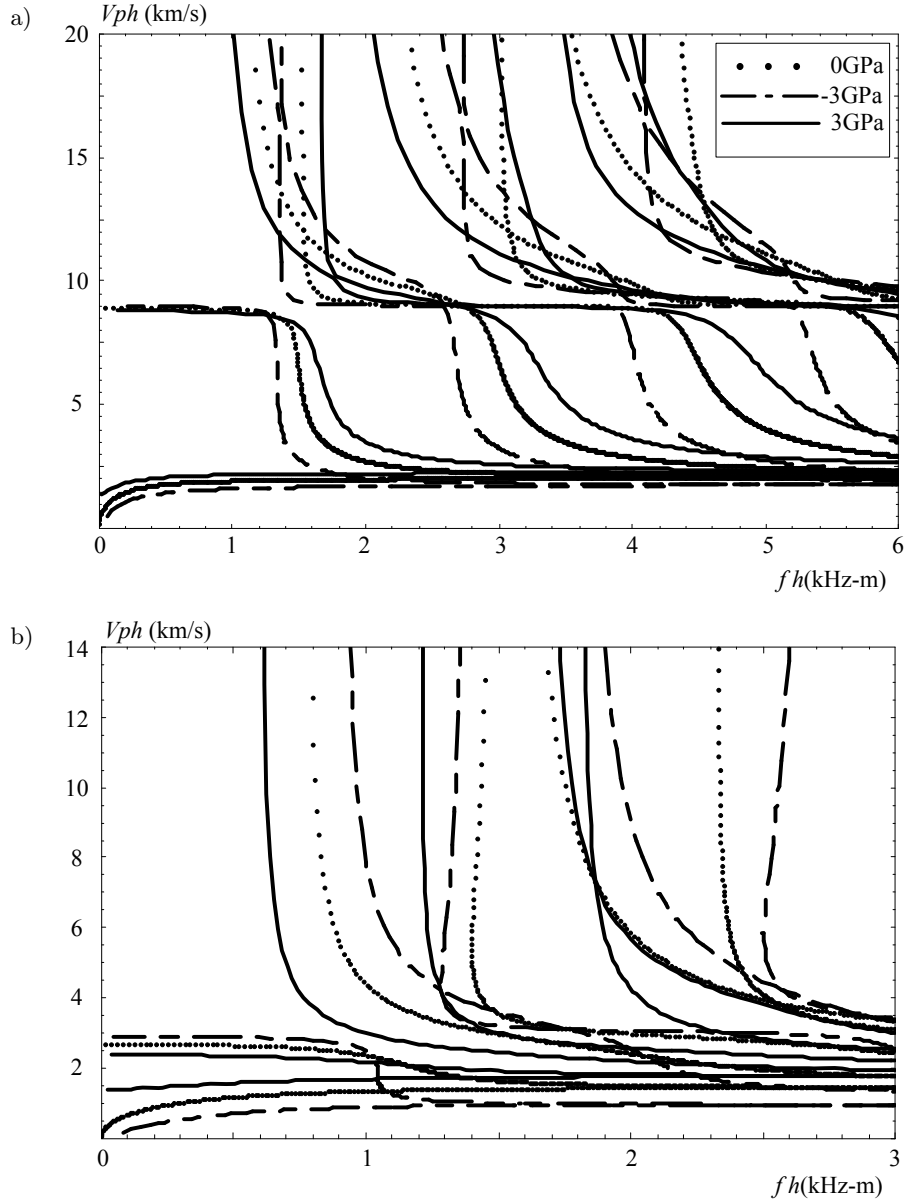


FIG. 5. Phase velocity spectra for the unidirectional plate under different homogeneous initial stresses Q : a) wave propagating in fiber orientation, b) wave propagating in the vertical fiber orientation.

$P = -3$ GPa and $P = -6(1 - z)$ GPa, of which the latter is inhomogeneous. The total stress of each case is equal to each other. It can be seen that the effect of the inhomogeneous initial stress is similar to that of the homogeneous initial

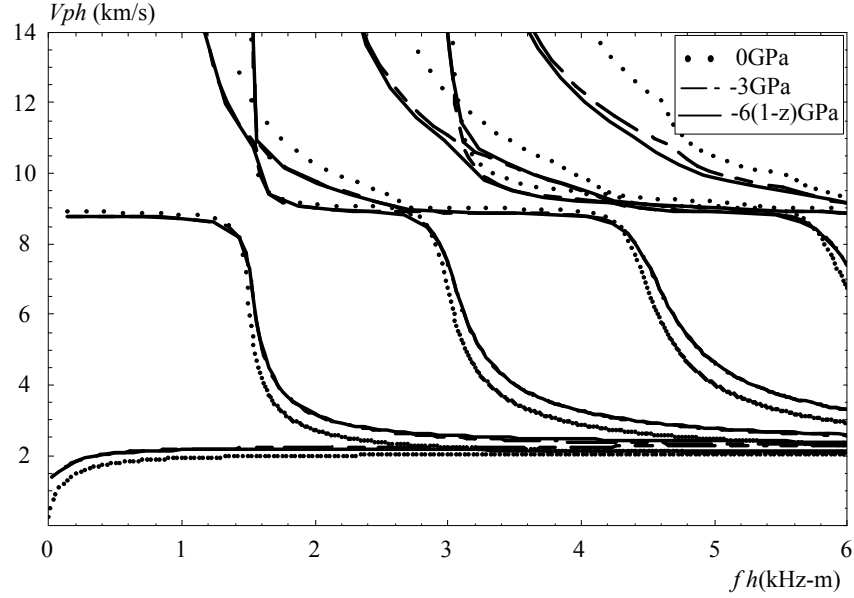


FIG. 6. Phase velocity spectra for the unidirectional plate with the wave propagating in fiber orientation under homogeneous and inhomogeneous initial stresses P .

stress at low order modes. However, as the mode order increases, the effect of the inhomogeneous initial stress becomes more significant.

Figures 7 and 8 illustrate the curves of frequency-initial stress P for the unidirectional plate with the wave respectively propagating in fiber orientation and the vertical fiber orientation.

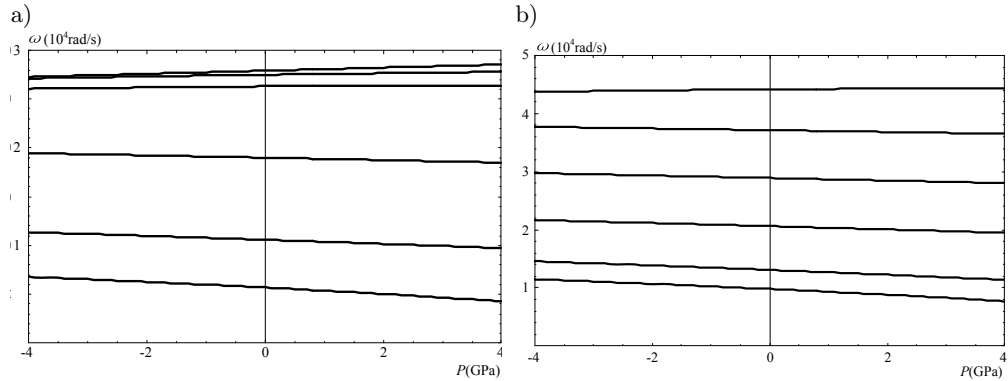


FIG. 7. Curves of frequency vs homogeneous initial stresses P for the unidirectional plate with the wave propagating in fiber orientation at: a) $kh = 3$, b) $kh = 5$.

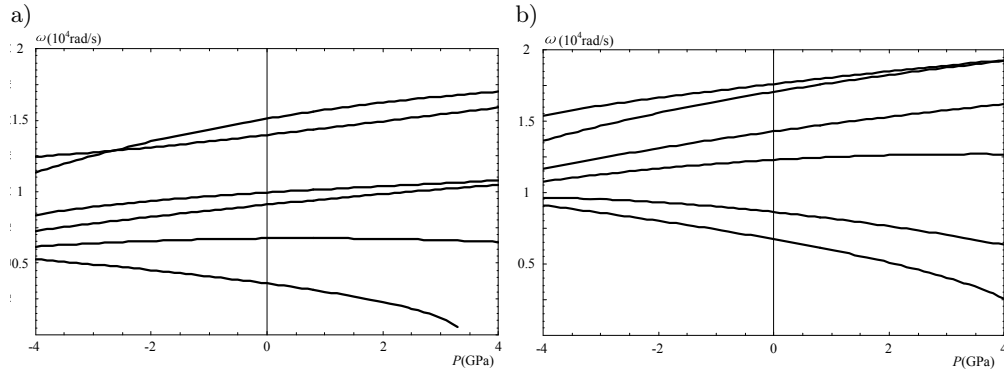


FIG. 8. Curves of frequency vs homogeneous initial stresses P for the unidirectional plate with the wave propagating in the vertical fiber orientation at: a) $kh = 3$, b) $kh = 5$.

Figures 9 and 10 are the curves of frequency-initial stress Q . It can be seen that the relations of frequency-initial stresses are approximately linear with the increasing of the initial stresses in both directions when the wave propagates in fiber orientation. But these relations are nonlinear and become more complicated when the wave propagates in the vertical fiber orientation. The varying trends of each mode are different. For different wavenumbers, the frequency varying curves are also different. The effects of the compressive stress and stretch stress are not always contrary. Like the second mode in Fig. 10c, the highest frequency is at about the initial stress $Q = 0$; both the compressive stress and stretch stress make the wave speed and frequency lower.

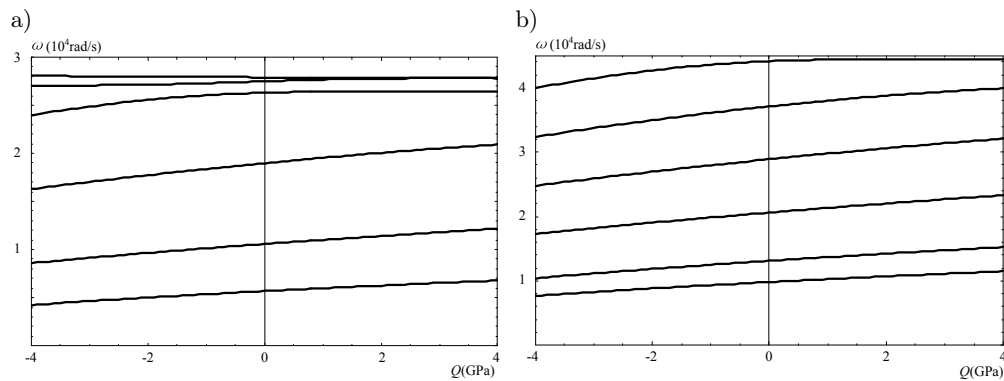


FIG. 9. Curves of frequency vs homogeneous initial stresses Q for the unidirectional plate with the wave propagating in fiber orientation at: a) $kh = 3$, b) $kh = 5$.

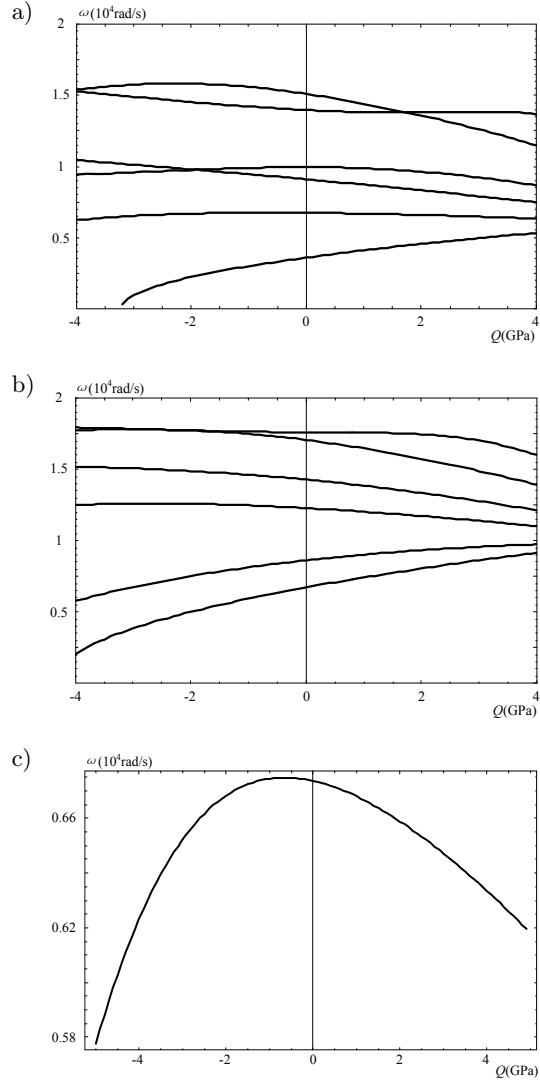


FIG. 10. Curves of frequency vs homogeneous initial stresses Q for the unidirectional plate with the wave propagating in the vertical fiber orientation: a) at $kh = 3$, b) at $kh = 5$, c) the second mode at $kh = 3$.

3.3. Effects of the initial stresses on the Lamb-like wave displacement and stress distributions

Figures 11 and 12 illustrate the displacement and stress distributions of the first three modes for the unidirectional plate with the wave propagating in fiber orientation under homogeneous initial stress $P = -3$ GPa and inhomogeneous

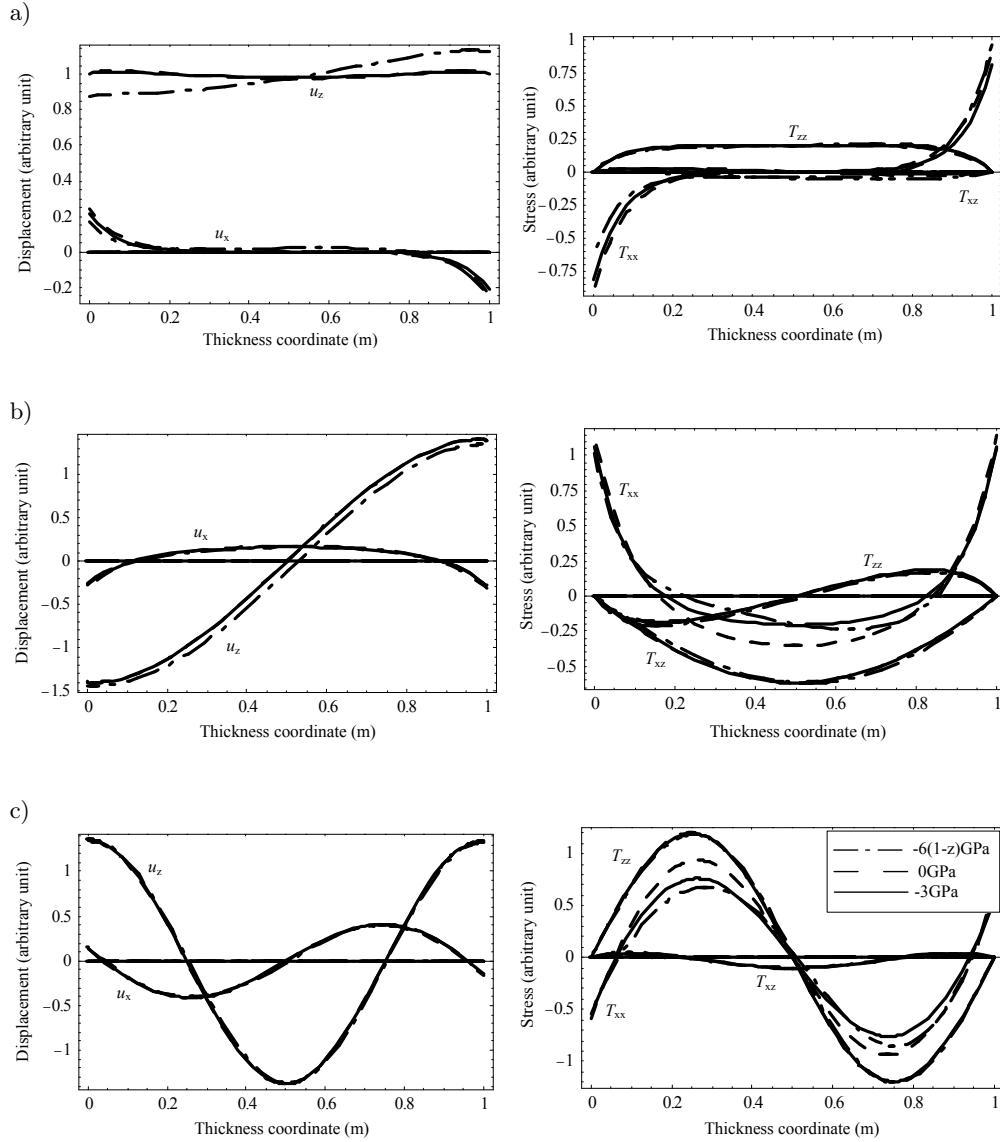


FIG. 11. Displacement and stress distributions for the unidirectional plate with the wave propagating in fiber orientation under different initial stresses P at $kh = 3$; a) the first mode, b) the second mode, c) the third mode.

initial stress $P = -6(1 - z)$ GPa at $kh = 3$ and $kh = 7$, respectively. It can be seen that the effects of the inhomogeneous initial stress are more significant both on the displacement distributions and on the stress distributions. The effect of the initial stress is strong on the T_{xx} stress distributions and weak on the T_{xz}

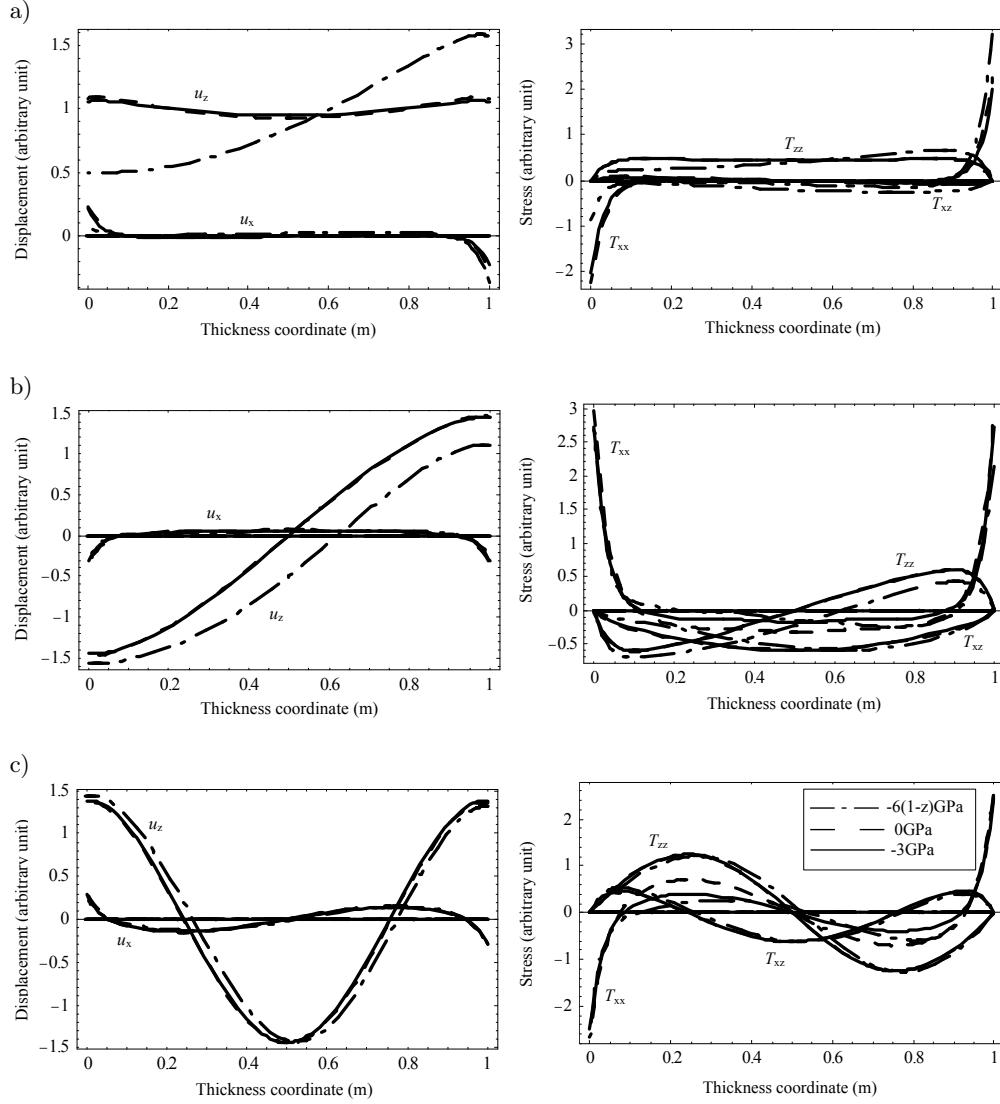


FIG. 12. Displacement and stress distributions for the unidirectional plate with the wave propagating in fiber orientation under different initial stresses P at $kh = 7$; a) the first mode, b) the second mode, c) the third mode.

and T_{zz} stress distributions. As the wavenumber increases, the effect of the initial stress becomes more significant.

Figure 13 illustrates the displacement and stress distributions of the first three modes for the unidirectional plate with the wave propagating in fiber orientation under homogeneous initial stress $Q = -3$ GPa at $kh = 3$. It can be

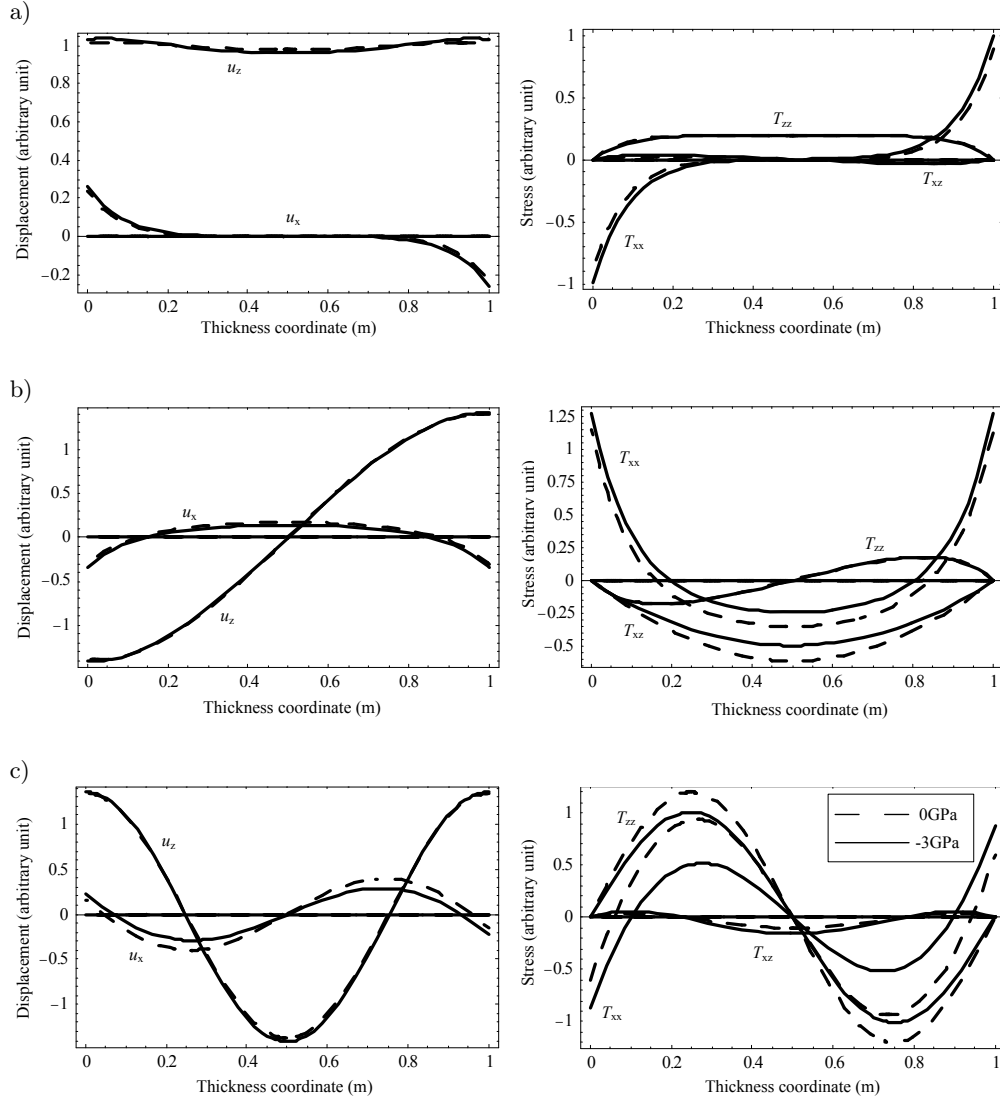


FIG. 13. Displacement and stress distributions for the unidirectional plate with the wave propagating in fiber orientation under initial stress Q at $kh = 3$; a) the first mode, b) the second mode, c) the third mode.

seen that the effect of the initial stress Q is strong on the T_{xx} and T_{xz} stress distributions and weak on the T_{zz} stress distributions. Comparing Fig. 13 with Fig. 11, we can see that the effects of the homogeneous initial stresses in different directions are different. In some cases, their effects are even contrary, such as the T_{xx} stress distributions at the first mode in Fig. 13a and Fig. 11a.

3.4. Effects of the initial stresses on the SH wave dispersion curves and displacement and stress distributions

Figures 14 and 15 show the dispersion curves for the unidirectional plate with the wave respectively propagating in fiber orientation and the vertical fiber orientation under different homogeneous initial stresses P . It can be seen that the effect of initial stress P is very regular. A compressive stress always makes the wave speed lower and a stretch stress makes the wave speed higher. The effect is weak at a little wavenumber and strong at a big wavenumber. The effect of initial stress P on the SH waves with the wave propagating in fiber orientation

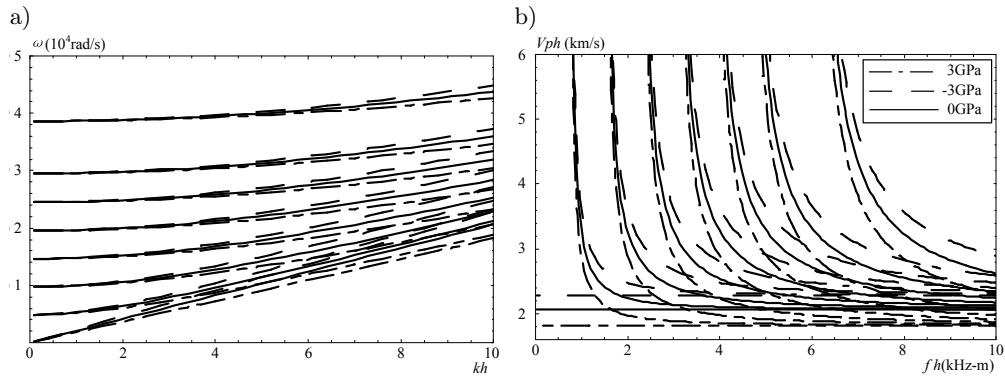


FIG. 14. Dispersion curves for the unidirectional plate with the wave propagating in fiber orientation under homogeneous initial stress P : a) frequency spectra, b) phase velocity spectra.

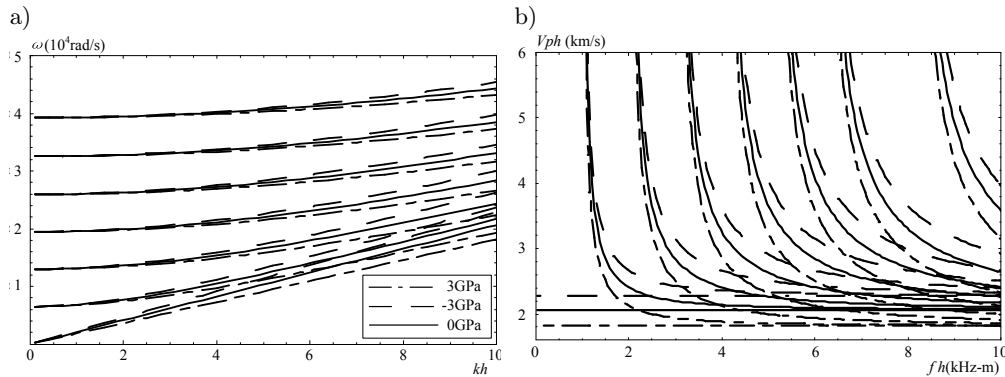


FIG. 15. Dispersion curves for the unidirectional plate with the wave propagating in the vertical fiber orientation under homogeneous initial stress P : a) frequency spectra, b) phase velocity spectra.

is similar to that with the wave propagating in the vertical fiber orientation. So, just the wave propagation in fiber orientation is discussed.

Figure 16 shows the dispersion curves for the unidirectional plate under homogeneous initial stress $P = -3$ GPa and inhomogeneous initial stress $P = -6(1 - z)$ GPa. It can be seen that the effect of inhomogeneous initial stress has little difference to that of homogeneous initial stress at high order modes, but the difference is significant at low order modes. As the wavenumber and frequency increase, the difference becomes more obvious.

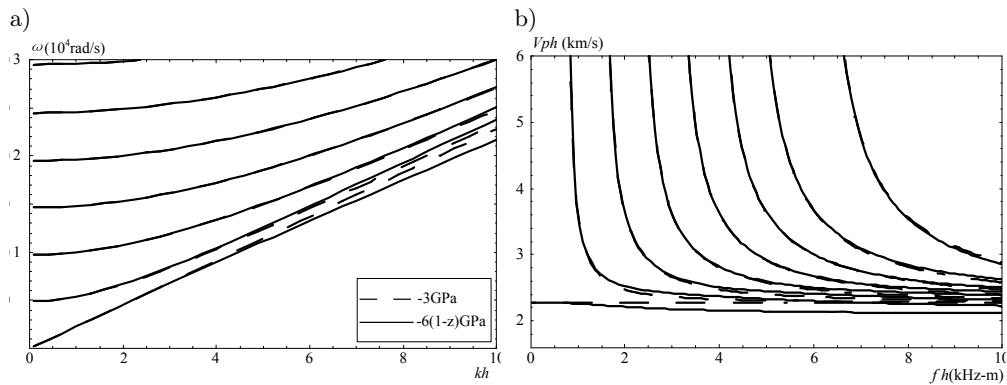


FIG. 16. Dispersion curves for the unidirectional plate under inhomogeneous initial stress P : a) frequency spectra, b) phase velocity spectra.

Figure 17 shows the dispersion curves for the unidirectional plate with the wave propagating in fiber orientation under different homogeneous initial stresses Q . It can be seen that the effect of initial stress Q is of some difference from that of initial stress P except that a compressive stress still makes the wave speed lower. The initial stress Q has almost no effect on the first mode, and for the other modes, the influence manner of the initial stress Q is different from that of the initial stress P .

Figure 18 illustrates the curves of frequency-initial stress P for the unidirectional plate with the wave propagating in fiber orientation. Figure 19 is the curves of frequency-initial stress Q . Comparing the two figures, we can see that the curves of frequency-initial stress P are sharp at low modes. With the wavenumber increasing, the curves become sharper for all modes. The effect of the compressive stress is entirely contrary to that of the stretch stress. With the increasing of the initial compressive stress, the frequencies approximately linearly become small. The curves of frequency-initial stress Q are sharp at high modes, which is very different from the curves of frequency-initial stress P . In particular, the frequency does not change with the variation of the initial stress at the first mode.

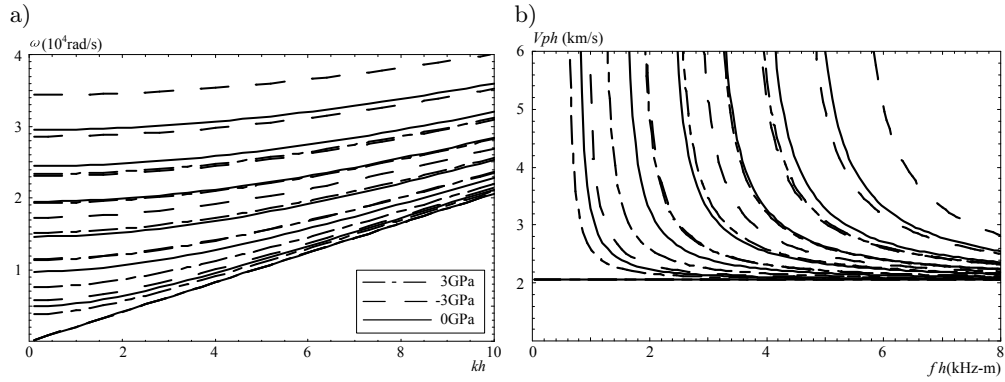


FIG. 17. Dispersion curves for the unidirectional plate under homogeneous initial stress Q : a) frequency spectra, b) phase velocity spectra.

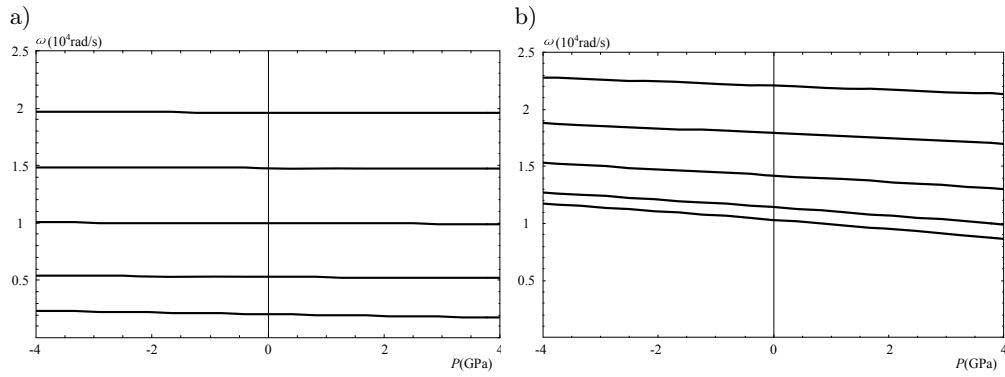


FIG. 18. Curves of frequency vs homogeneous initial stresses P for the unidirectional plate at: a) $kh = 3$, b) $kh = 5$.

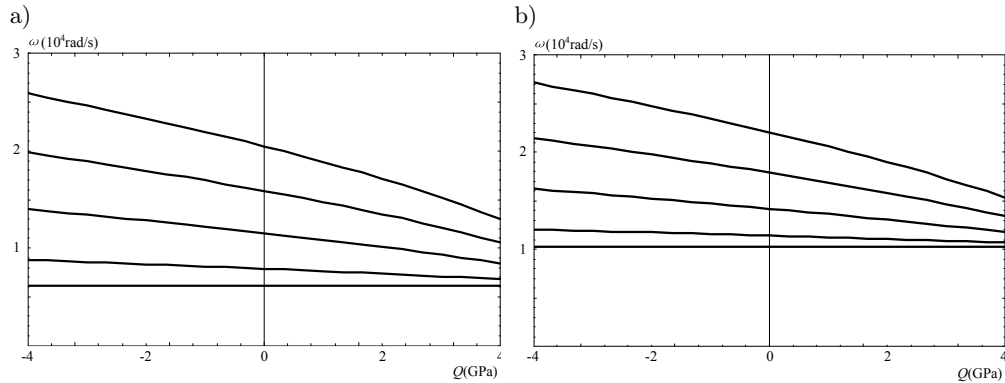


FIG. 19. Curves of frequency vs homogeneous initial stresses Q for the unidirectional plate at: a) $kh = 3$, b) $kh = 5$.

Figure 20 illustrates the displacement and stress distributions of the lower modes for the unidirectional plate with the wave propagating in fiber orientation under homogeneous initial stress $P = -3$ GPa and inhomogeneous initial stress $P = -6(1 - z)$ GPa at $kh = 5$. It can be seen that the homogeneous initial stress has almost no effect on the displacement and stress distributions. The inhomogeneous initial stress has significant effects on the displacement and stress distributions, which is more obvious at the first order mode.

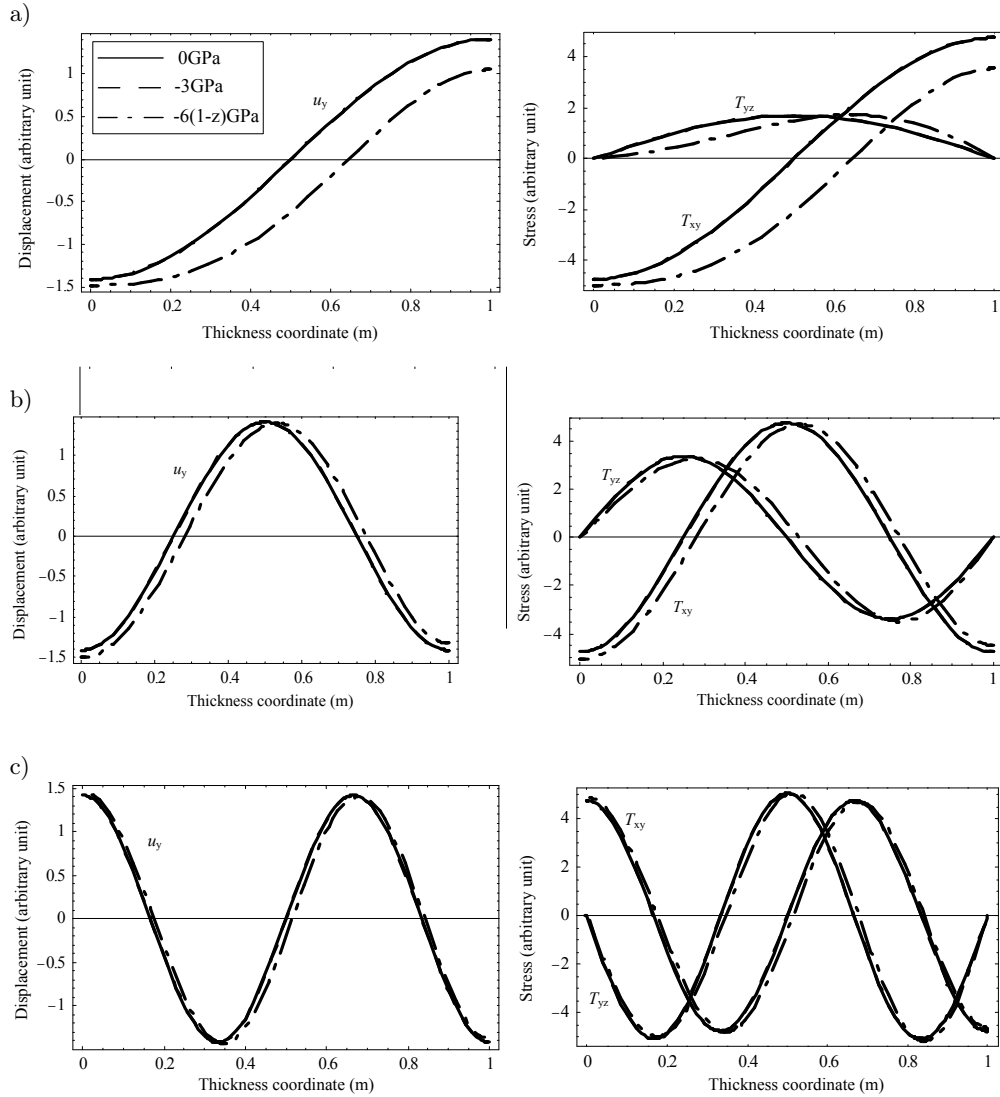


FIG. 20. Displacement and stress distributions of the unidirectional plate under different initial stresses P at $kh = 5$; a) the second mode, b) the third mode, c) the fourth mode.

4. Conclusions

In this paper, we use the Legendre polynomial series method to solve the guided wave propagation in unidirectional plates under gravity, homogeneous initial stresses in the thickness direction and inhomogeneous initial stresses in the wave propagating direction. The effects of the initial stress on the dispersion curves, displacement and stress distributions are illustrated. Based on the calculated results, the following conclusions can be drawn:

1. The effect of the initial stress on the Lamb-like waves is quite different from that on the SH waves. The effect on SH waves is very regular.
2. For Lamb-like waves, the effect of the initial stress in the thickness direction on the symmetrical modes is different from that on the anti-symmetrical modes when the wave propagates in fiber orientation.
3. For Lamb-like waves, the effect of the initial stress in the thickness direction is usually different from that in the wave propagation direction.
4. For Lamb-like waves, the relations of frequency-initial stresses are nonlinear when the wave propagates in the vertical fiber orientation.
5. For Lamb-like waves, the effect of the compressive stress is not always contrary to that of the stretch stress. For SH waves, the effect of the compressive stress is entirely contrary to that of the stretch stress except for the first mode.
6. For Lamb-like waves, the effects of the initial stresses in different directions on the displacement and stress distributions are different and are even contrary in some cases. For SH waves, the homogeneous initial stresses have very weak effects on the displacement and stress distributions.

Acknowledgment

The work was supported by the National Natural Science Foundation of China (No. 11272115) and Foundation for University Key Teacher of He'Nan Province of China (No.2011GGJS055) and by the high-performance grid computing platform of Henan Polytechnic University.

Appendix

The elements of the matrices in Eq. (2.11) are given by

$$A_{11}^{j,m} = [C_{55} + 0.5(P - Q)]U(m, j, 0, 2) + 0.5P'u(m, j, 0, 1) \\ - k^2(C_{11} + P)u(m, j, 0, 0) + C_{55}k(m, j, 0, 1),$$

$$\begin{aligned}
A_{12}^{j,m} &= ik[(C_{55} + C_{13} + 0.5(P + Q))u(m, j, 0, 1) \\
&\quad + (0.5P' + \rho g)u(m, j, l, 0) + C_{55}k(m, j, 0, 0)], \\
A_{21}^{j,m} &= ik[(C_{55} + C_{13} + 0.5(P + Q))u(m, j, 0, 1) \\
&\quad - \rho g u(m, j, 0, 0) + (C_{13} + Q)k(m, j, 0, 0)], \\
A_{22}^{j,m} &= (C_{33} + Q)u(m, j, 0, 2) - k^2(C_{55} - 0.5P + 0.5Q)u(m, j, 0, 0) \\
&\quad + (C_{33} + Q)k(m, j, 0, 1), \\
M_m^j &= u(m, j, 0, 0),
\end{aligned}$$

where

$$\begin{aligned}
u(m, j, n, l) &= \int_0^h Q_j^*(z) z^n \frac{\partial^l Q_m(z)}{\partial z^l} dz, \\
k(m, j, n, l) &= \int_0^h Q_j^*(z) z^n \frac{\partial \pi(z)}{\partial z} \frac{\partial^l Q_m(z)}{\partial z^l} dz.
\end{aligned}$$

References

1. M.A. BIOT, *Mechanics of Incremental Deformations*, John Wiley & Sons, Inc., New York, 1965.
2. S. DEY, *Wave propagation in two layered medium under initial stresses*, Pure Appl. Geophys., **90**, 38–52, 1971.
3. J.P. JONES, *Wave propagation in a two layered medium*, J. Appl. Mechanics, **E31**, 213–222, 1964.
4. P.P. ROY, *Wave propagation in a thinly two layered medium with stress couples under initial stresses*, Acta Mechanica, **54**, 1–21, 1984.
5. A.M. ABD-ALLA, S.M. AHMED, *Propagation of Love waves in a non-homogeneous orthotropic elastic layer under initial stress overlying semi-infinite medium*, Applied Mathematics and Computation, **106**, 265–275, 1999.
6. G. NEETU, *Effect of initial stress on harmonic plane homogeneous waves in viscoelastic anisotropic media*, J. Sound Vib., **303**, 3–5, 515–25, 2007.
7. A. MONTANARO, *Wave propagation along axes of symmetry in linear elastic media with initial stress*, J. Elasticity, **46**, 217–221, 1997.
8. A.S. GUZ, *Elastic waves in compressible materials with initial stress and a nondestructive ultrasonic method for the determination of biaxial residue stresses*, Int. Appl. Mech., **30**, 1–14, 1994.
9. S.D. AKBAROV, M. OZISIK, *The influence of the third order elastic constants to the generalized Rayleigh wave dispersion in a pre-stressed stratified half-plane*, International Journal of Engineering Science, **41**, 2047–2061, 2003.

10. S. GUPTA, D.K. MAJHI, S. KUNDU, S.K. VISHWAKARMA, *Propagation of torsional surface waves in a homogeneous layer of finite thickness over an initially stressed heterogeneous half-space*, Applied Mathematics and Computation, **218**, 5655–5664, 2012.
11. B. SINGH, *Wave propagation in a prestressed piezoelectric half-space*, Acta Mechanica, **211**, 337–3344, 2010.
12. S.D. AKBAROV, M.S. GULIEV, *Axisymmetric longitudinal wave propagation in a finite pre-strained compound circular cylinder made from compressible materials*, CMES: Computer Modeling in Engineering and Sciences, **39**, 2, 155–177, 2009.
13. S.D. AKBAROV, T. KEPCELER, M.M. EGILMEZ, *Torsional wave dispersion in a finitely pre-strained hollow sandwich circular cylinder*, Journal of Sound and Vibration, **330**, 4519–4537, 2011.
14. S.D. AKBAROV, M.S. GULIEV, *The influence of the finite initial strains on the axisymmetric wave dispersion in a circular cylinder embedded in a compressible elastic medium*. International Journal of Mechanical Sciences, **52**, 89–95, 2010.
15. P. KAYESTHA, A.C. WIJEYEWICKREMA, *Time-harmonic wave propagation in a pre-stressed compressible elastic bi-material laminate*, European Journal of Mechanics A/Solids **29**, 143–151, 2010.
16. S.D. AKBAROV, A.D. ZAMANOV, E.R. AGASIYEV, *On the propagation of Lamb waves in a sandwich plate made of compressible materials with finite initial strains*, Mechanics of Composite Materials, **44**, 2, 155–164, 2008.
17. A.D. ZAMANOV, E.R. AGASIYEV, *Dispersion of lamb waves in a three-layer plate made from compressible materials with finite initial deformations*, Mechanics of Composite Materials, **46**, 6, 583–592, 2011.
18. S.D. AKBAROV, E.R. AGASIYEV, A.D. ZAMANOV, *Wave propagation in a pre-strained compressible elastic sandwich plate*, European Journal of Mechanics A/Solids, **30**, 409–422, 2011.
19. M.M. SELIM, M.K. AHMED, *Plane strain deformation of an initially stressed orthotropic elastic medium*, Applied Mathematics and Computation, **175**, 221–237, 2006.
20. J.L. ROSE, *Ultrasonic Waves in Solid Media*, Cambridge University Press, Cambridge, UK, 1999.

Received July 6, 2012; revised version November 2, 2012.
